# DOMAIN REDUCTION METHOD FOR SINGLE AND TWO-PHASE DYNAMIC SOIL-STRUCTURE INTERACTION PROBLEMS

Andrzej Truty
*Department of Environmental Engineering, Cracow University of Technology, Cracow,Poland*

Thomas Zimmermann
*Zace services Ltd, Lausanne, Switzerland*

**ABSTRACT:** *Transient dynamic soil-structure time history analyses for single or two-phase fully or partially saturated media require appropriate techniques for correct representation of boundary conditions and inclusion of the free field motion into the model. Size of the computational model is frequently a serious limitation in practical applications. One of the approaches that allows to reduce computational effort is the domain reduction method (DRM) formulated first by Bielak et.al. (Bielak, Loukakis, Hisada, & Youshimura 2003),(Youshimura, Bielak, Hisada, & Fernandez 2003), for single phase, later on extended to the two-phase fully saturated media by Kantoe et al. (Kantoe 2006). In this paper an implicit DRM method is proposed for two-phase fully or partially saturated media, extending the theory given by Aubry and Ozanam (Aubry & Ozanam 1988) (for static consolidation), using a stabilized (through pressure Laplacian) u-p formulation (Truty & Zimmermann 2006) worked out for low order 2D/3D BBAR and EAS elements. Numerical results for twin shallow tunnels subject to the Loma Prieta earthquake show robustness of the method.*

## 1 INTRODUCTION

Nonlinear dynamic time history analyses using FE models put certain restrictions on size of elements, time step and size of the domain adjacent to the structure. Spurious wave reflections usually result from the truncation of the FE model, even if special viscous boundaries are used. Also when the source of the excitation is far from the structure or is nonuniform the computational model may become extremely large and therefore computationally inefficient. To overcome this difficulty Bielak et.al. (Bielak, Loukakis, Hisada, & Youshimura 2003),(Youshimura, Bielak, Hisada, & Fernandez 2003) proposed a two step procedure called domain reduction method (DRM), for single-phase media, which allows to move source of the excitation to a smaller domain relatively close to the structure and thus to reduce the size of the computational model. In 2006 Kantoe (Kantoe 2006), and later Kantoe et al.(Kantoe, Zdravkovic, & Potts 2008) published an implicit DRM formulation for dynamic consolidation of fully saturated media. Although full saturation is the most interesting case for engineering practice, we still have to deal, in many cases, with media that are partially saturated (earth dams etc..). In this paper we will briefly describe the set of equations governing dynamic consolidation of two-phase partially saturated media and present major steps to derive the corresponding DRM formulation. Contrary to the work by Kantoe the DRM model is derived in a semi-discrete form that allows to apply any suitable time integration scheme to the momentum and fluid mass balance equations. Efficiency of the method is tested on the problem of twin tunnels subjected to a scaled Loma Prieta earthquake acceleration record.

## 2 GOVERNING EQUATIONS FOR TWO-PHASE DYNAMIC CONSOLIDATION

Based on static formulation by Aubry and Ozanam (Aubry & Ozanam 1988) the two-phase dynamic consolidation of fully or partially saturated media, designed for the $u-p$ format, can be written as the following set of differential equations and corresponding boundary and initial conditions.

- overall equilibrium equation for the solid and fluid phases written in terms of the total stress

$$\sigma^{\text{tot}}_{ij,j} + \rho\, g\, b_i = \rho\, \ddot{u}_i \tag{1}$$

$$\rho = \rho_{\text{dry}} + n\, S\, \gamma^{\text{F}} \tag{2}$$

  where total stress is denoted by $\sigma^{\text{tot}}_{ij}$, earth acceleration by $g$, solid skeleton bulk density by $\rho_{\text{dry}}$, water specific weight by $\gamma^F$, porosity by $n$ and current saturation ratio by $S$
- extended effective stress principle after Bishop

$$\sigma^{\text{tot}}_{ij} = \sigma_{ij} + \delta_{ij}\ S\ p \tag{3}$$

  where Kronecker's symbol is denoted by $\delta_{ij}$, effective stresses by $\sigma_{ij}$ and pore pressure by $p$
- fluid flow continuity equation including the effect of compressibility of the fluid and partial saturation

$$S\,\dot{\varepsilon}_{kk} + v^{\text{F}}_{k,k} = \left( n\frac{S}{K^F} + n\,\frac{\partial S}{\partial p} \right)\ \dot{p} \tag{4}$$

  where $k-$th component of Darcy velocity vector is denoted by $v^F_k$, while fluid bulk modulus by $K^F$
- linearized strain-displacement relations

$$\varepsilon_{ij} = \frac{1}{2}\,(u_{i,j} + u_{j,i}) \tag{5}$$

  where engineering strain is denoted by $\varepsilon_{ij}$ and $i-$th component of displacement vector is denoted by $u_i$
- nonlinear elasto-plastic constitutive relation

$$\dot{\sigma}_{ij} = D^{\text{e}}_{ijkl}\,(\dot{\varepsilon}_{kl} - \dot{\varepsilon}^{\text{p}}_{kl}) \tag{6}$$

  where $D_{ijkl}$ denotes $ijkl$ component of fourth-order current elasticity tensor and $\dot{\varepsilon}_{kl}$, $\dot{\varepsilon}^{\text{p}}_{kl}$ denote rates of total and plastic strains respectively.
- extended Darcy's law (including optionally the inertial term)

$$v^F_i = k_{ij} k_r(S) \left( \frac{1}{\gamma^F} p_{,j} + b_j - \frac{1}{g}\ddot{u}_j \right) \tag{7}$$

- simplified constitutive equations for saturation ratio $S$, after van Genuchten (Genuchten 1980), and relative permeability coefficient $k_r(S)$ after Irmay (Irmay 1956)

$$S = S(p) = \left\{ \begin{array}{ll} S_r + \dfrac{1 - S_r}{\left[ 1 + \left( \alpha \dfrac{p}{\gamma_{\text{F}}} \right)^2 \right]^{1/2}} & \text{if } p > 0 \\ 1 & \text{if } p \leq 0 \end{array} \right\} \tag{8}$$

$$k_r\left(S\right)=\left(\frac{S-S_r}{1-S_r}\right)^3 \tag{9}$$

where the residual saturation ratio is denoted by $S_r$, and $\alpha$ is a material parameter responsible for a decrease of a saturation ratio with an increase of a pressure suction

- near field boundary conditions to be satisfied at any time $t \in [0,T]$

$$\sigma_{ij}^{\text{tot}} n_j = \overline{t_i} \text{ on } \Gamma_{\text{t}} \quad ; v_i^{\text{F}} n_i = \overline{q} \text{ on } \Gamma_{\text{q}} \quad ; u_i = \overline{u}_i \text{ on } \Gamma_{\text{u}} \quad ; p = \overline{p} \text{ on } \Gamma_{\text{p}} \tag{10}$$

  $\Gamma_{\text{t}}$, $\Gamma_{\text{q}}$, $\Gamma_{\text{u}}$, $\Gamma_{\text{p}}$ are parts of the boundary where the total stresses, fluid fluxes, displacements and pore pressures are prescribed.
  A special treatment is required for so-called *seepage surface* where the free surface intersects with domain boundary, see (Aubry & Ozanam 1988) for details.
- farfield boundary conditions
  To analyze truncated FE models, a zeroth-order paraxial absorbing boundary formulation (coherent with the u-p format), proposed by Modaressi and Bonzenati (Modaressi & Benzenati 1994), is extended here to handle partial saturation in a simplified manner. The total viscous stress and fluid flux, on the absorbing boundary, are defined as follows

$$\sigma_i^s = -\left\{\rho\frac{c_p^2}{V_{p1}}\left(\lambda_s+2\mu_s\right)n_i n_j + \rho\, c_s\left(t_{1i}t_{1j}-t_{2i}t_{2j}\right)\right\}v_j^s + n_i\left(S\,p - S_o\,p_o\right) \tag{11}$$

$$\Phi = k\left[\rho\left(1-\frac{c_p^2}{V_{p1}^2}-\rho^F\right)\right]n_k a_k^s \tag{12}$$

  The corresponding shear and dilatational wave velocities, for solid phase, are defined through the expressions

$$c_s=\sqrt{\frac{G}{\rho}} \qquad c_p=\sqrt{\frac{\lambda+2\,G}{\rho}} \tag{13}$$

  while the approximate first dilatational wave velocity for medium filled by a compressible fluid is defined as

$$V_{p1}^2 = c_p^2\left(1+\frac{Q}{\lambda+2\,G}\right) \tag{14}$$

  and

$$\frac{1}{Q} = n\frac{S}{K^F} + n\frac{dS}{dp} \tag{15}$$

  Components of solid velocity and acceleration vectors are denoted by $v_i^s$ and $a_i^s$. Normalized components of normal and tangential vectors are denoted by $n_i$ and $t_{1i}$, $t_{2i}$ respectively. In the expression for the total viscous stress the $S_o\,p_o$ term is added to cancel the initial saturation/pressure prior to running dynamic time history analysis. The $\frac{dS}{dp}$ term is computed using van Genuchten's law while $k$ is the permeability value along the normal direction. It has to be mentioned that this formulation is only approximate and hence spurious reflections are not fully eliminated. For single-phase media expressions given above correspond to well known Lysmer viscous dashpots.
- initial conditions

$$u_i(t=t_o)=u_{io} \quad ; \quad p(t=t_o)=p_o \tag{16}$$

### 2.1 Semi-discrete form of balance equations

In the following derivations the $\mathrm{HHT}_\alpha$ implicit schemes are used fulfilling unconditional stability. The $\mathrm{HHT}_\alpha$ scheme nicely damps high frequencies without disturbing low ones.

The following expressions (Zienkiewicz, Chan, Pastor, Schrefler, & Shiomi 1999), (Hilber, Hughes, & Taylor 1977) are used to integrate solid displacements, velocities and pore pressures in time

$$\mathbf{u}_{n+1} = \mathbf{u}_n + \dot{\mathbf{u}}_n \Delta t + \frac{\Delta t^2}{2}\left[(1-2\beta)\,\ddot{\mathbf{u}}_n + 2\beta\ddot{\mathbf{u}}_{n+1}\right] \tag{17}$$

$$\dot{\mathbf{u}}_{n+1} = \dot{\mathbf{u}}_n + \Delta t\left[(1-\gamma)\,\ddot{\mathbf{u}}_n + \gamma\ddot{\mathbf{u}}_{n+1}\right] \tag{18}$$

$$p_{n+1} = p_n + (1-\theta)\,\dot{p}_n\Delta t + \theta\Delta t\dot{p}_{n+1} \tag{19}$$

with

$$-\frac{1}{3} \le \alpha < 0,\;\; \gamma = \frac{(1-2\alpha)}{2},\;\; \beta = \frac{(1-\alpha)^2}{4},\;\; \theta \ge \frac{1}{2} \tag{20}$$

The resulting semi-discrete matrix form of the overall equilibrium in the HHT scheme can be written as follows

$$\mathbf{M}\ddot{\mathbf{u}}_{n+1} + \mathbf{C}\dot{\mathbf{u}}_{n+\alpha} + \mathbf{F}'_{\text{int}}(\mathbf{u}_{n+\alpha}) + \mathbf{C}^F\mathbf{p}_{n+\alpha} = \mathbf{F}_{\text{ext}n+\alpha} \tag{21}$$

To preserve symmetry of the resulting matrix form (if we neglect the inertial term in the Darcy law) the semi-discrete matrix form of balance of the mass for the fluid phase is written at $t_{n+\alpha}$

$$\left(\mathbf{C}^F\right)^{\mathrm{T}}\dot{\mathbf{u}}_{n+\alpha} - \mathbf{H}^F\,\mathbf{p}_{n+\alpha} + \mathbf{R}^F\ddot{u}_{n+\alpha} - \mathbf{h}^F - \mathbf{M}^F\dot{\mathbf{p}}_{n+\alpha} + \mathbf{Q}^F = \mathbf{0} \tag{22}$$

where

$$\mathbf{F}'_{int}(\mathbf{u}_{n+\alpha}) = \int_\Omega \mathbf{B}^{\mathrm{T}}\boldsymbol{\sigma}(\mathbf{u}_{n+\alpha})\mathrm{d}\Omega \tag{23}$$

$$\mathbf{C}^F = \int_\Omega \mathbf{N}^{\mathrm{T}} S_{n+\alpha}\mathbf{1}^{\mathrm{T}}\mathrm{d}\Omega \tag{24}$$

$$\mathbf{H}^F = \frac{1}{\gamma^F}\int_\Omega \nabla\mathbf{N}^{\mathrm{T}}\mathbf{k}\nabla\mathbf{N}\mathrm{d}\Omega \tag{25}$$

$$\mathbf{M}^F = \int_\Omega \mathbf{N}^{\mathrm{T}} c_{n+\alpha}\mathbf{N}\mathrm{d}\Omega \tag{26}$$

$$\mathbf{R}^F = \int_\Omega \nabla\mathbf{N}^{\mathrm{T}}\mathbf{k}\frac{1}{g}\mathbf{N}\mathrm{d}\Omega \tag{27}$$

$$\mathbf{h}^F = \int_\Omega \nabla\mathbf{N}^{\mathrm{T}}\mathbf{k}\mathbf{b}\mathrm{d}\Omega \tag{28}$$

$$\mathbf{Q}^F = \int_{\Gamma_q} \mathbf{N}^{\mathrm{T}}\overline{q}\mathrm{d}\Omega \tag{29}$$

In the above expressions matrices of the standard shape functions are denoted by **N**, strain-displacement operator by **B**, normalized gravity direction vector by **b**, current permeability matrix by **k**, storage coefficient $c_{n+\alpha} = c(p_{n+\alpha}) = n\left(\frac{S_{n+\alpha}}{K^F} + \frac{dS_{n+\alpha}}{dp}\right)$, $g$ is an earth acceleration

($g$=9.81 m/s$^2$), and imposed fluid flux at boundary $\Gamma_q$ is denoted by $\overline{q}$. In order to reduce computational complexity we assume that all matrices in fluid mass balance equation are treated in an explicit manner. It has to be mentioned that within ZSOIL code (Elmepress and Zace Services Limited 2013) low order elements (BBAR or EAS) are exclusively used, hence equal interpolation order for displacement and pressure degrees of freedom is the only choice. This setting may yield spurious spatial pressure oscillations in the incompressibility limit, and for that reason a special stabilization procedure, based on pressure Laplacian, is used to circumvent this deficiency (the same as for the standard static consolidation problems) (Truty & Zimmermann 2006).

## 3 DRM METHOD FOR SINGLE AND TWO-PHASE PARTIALLY SATURATED MEDIA

The goal of DRM method is to reduce the size of the the computational model to the structure and only a small adjacent part of the subsoil. Let us consider a domain that includes a fault, source of the excitation forces $\mathbf{P}_e(t)$, and a structure (see Fig.1(a)). At this point we may analyze two computational models. The first one, called "background model" (see Fig.1(b)), includes subsoil and source of the load $\mathbf{P}_e(t)$, while the second one, called "reduced model" (see Fig.1(c)), includes the structure and a small part of the subsoil. Zone between $\Gamma$ and $\Gamma^+$ consists of a single row of finite elements while $\tilde{\Omega}^+$ is only a part of the exterior domain $\Omega^+$ placed outside of $\Gamma$.

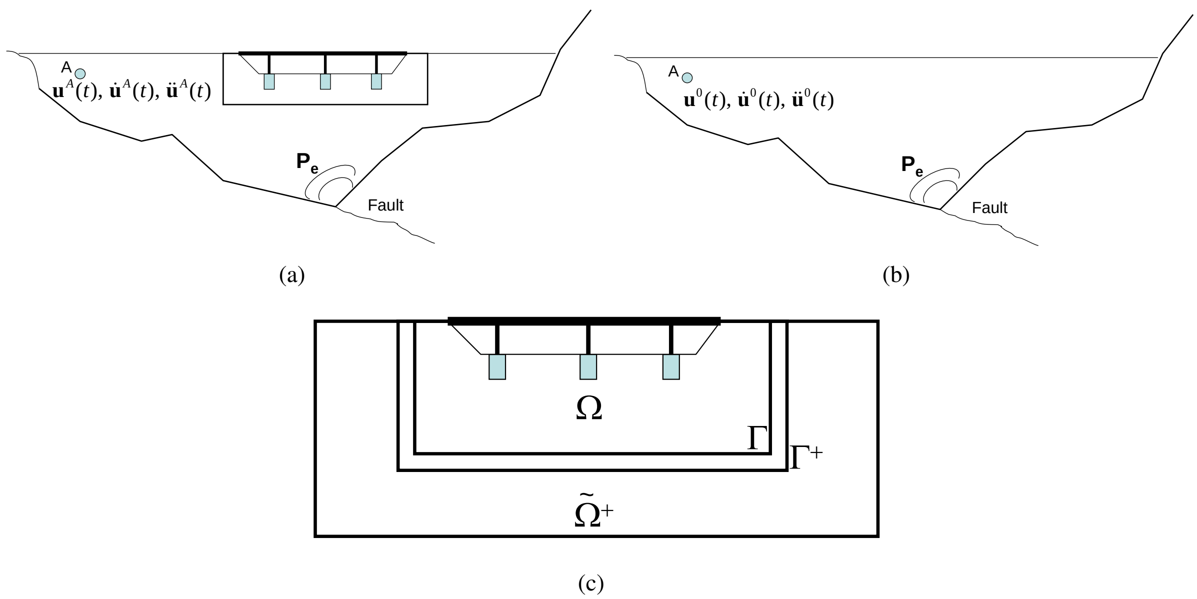


Fig. 1. General idea of DRM method. (a) Full model of subsoil, structure, and source of the loading $\mathbf{P}_e(t)$. (b) Background model. (c) Reduced model.

By solving the background model one may compute the free field motion induced by $\mathbf{P}_e(t)$. Resulting free field displacements, velocities, accelerations, pore pressures and pore pressure rates are denoted by $u^0(t)$, $\dot{u}^0(t)$, $\ddot{u}^0(t)$, $p^0(t)$, $\dot{p}^0(t)$ respectively. The background model is partitioned into interior domain $\Omega$ and the exterior one $\Omega^+$. The $\Gamma$ boundary separates interior and exterior domains. The free field quantities at any point in the interior domain are denoted using index $()_i$, at the boundary $\Gamma$ with index $()_b$ and in the exterior domain using index $()_e$. Nodal points that belong to the boundary $\Gamma$ are labeled as $b$, nodes that are in the $\Omega^+$ domain and do not belong to the boundary $\Gamma$ are labeled as $e$, and the remaining ones as $i$. For the sake of simplicity damping (in overall equilibrium) and stabilization term (in the fluid mass balance) are neglected here (adding these terms is straightforward).

After partitioning the domain into $\Omega$ and $\Omega^+$ one may write equations of overall equilibrium (eq.30), (eq.31) and fluid mass balance (eq.32), (eq.33) in $\Omega$ and $\Omega^+$ respectively ($\mathbf{P}_b$, $\mathbf{Q}_b$ represent boundary forces/fluxes along $\Gamma$ while $\mathbf{P}_e$, $\mathbf{Q}_e$ excitation forces/fluxes).

- Overall equilibrium in $\Omega$

$$\begin{bmatrix} \mathbf{M}_{ii}^{\Omega} & \mathbf{M}_{ib}^{\Omega} \\ \mathbf{M}_{bi}^{\Omega} & \mathbf{M}_{bb}^{\Omega} \end{bmatrix} \begin{Bmatrix} \ddot{\mathbf{u}}_i \\ \ddot{\mathbf{u}}_b \end{Bmatrix} + \begin{Bmatrix} \mathbf{F}'_{int_i} \\ \mathbf{F}'_{int_b} \end{Bmatrix} + \begin{bmatrix} \mathbf{C^F}_{ii}^{\Omega} & \mathbf{C^F}_{ib}^{\Omega} \\ \mathbf{C^F}_{bi}^{\Omega} & \mathbf{C^F}_{bb}^{\Omega} \end{bmatrix} \begin{Bmatrix} \mathbf{p}_i \\ \mathbf{p}_b \end{Bmatrix} = \begin{Bmatrix} \mathbf{0} \\ \mathbf{P_b} \end{Bmatrix} \tag{30}$$

- Overall equilibrium in $\Omega^+$

$$\begin{bmatrix} \mathbf{M}_{bb}^{\Omega+} & \mathbf{M}_{be}^{\Omega+} \\ \mathbf{M}_{eb}^{\Omega+} & \mathbf{M}_{ee}^{\Omega+} \end{bmatrix} \begin{Bmatrix} \ddot{\mathbf{u}}_b \\ \ddot{\mathbf{u}}_e \end{Bmatrix} + \begin{Bmatrix} \mathbf{F}'_{int_b} \\ \mathbf{F}'_{int_e} \end{Bmatrix} + \begin{bmatrix} \mathbf{C^F}_{bb}^{\Omega+} & \mathbf{C^F}_{be}^{\Omega+} \\ \mathbf{C^F}_{eb}^{\Omega+} & \mathbf{C^F}_{ee}^{\Omega+} \end{bmatrix} \begin{Bmatrix} \mathbf{p}_b \\ \mathbf{p}_e \end{Bmatrix} = \begin{Bmatrix} -\mathbf{P}_b \\ \mathbf{P}_e \end{Bmatrix} \tag{31}$$

- Fluid mass balance in $\Omega$

$$\begin{aligned} &\begin{bmatrix} \mathbf{R^F}_{ii}^{\Omega} & \mathbf{R^F}_{ib}^{\Omega} \\ \mathbf{R^F}_{bi}^{\Omega} & \mathbf{R^F}_{bb}^{\Omega} \end{bmatrix} \begin{Bmatrix} \ddot{\mathbf{u}}_i \\ \ddot{\mathbf{u}}_b \end{Bmatrix} + \begin{bmatrix} \left(\mathbf{C^F}_{ii}^{\Omega}\right)^{\mathrm{T}} & \left(\mathbf{C^F}_{ib}^{\Omega}\right)^{\mathrm{T}} \\ \left(\mathbf{C^F}_{bi}^{\Omega}\right)^{\mathrm{T}} & \left(\mathbf{C^F}_{bb}^{\Omega}\right)^{\mathrm{T}} \end{bmatrix} \begin{Bmatrix} \dot{\mathbf{u}}_i \\ \dot{\mathbf{u}}_b \end{Bmatrix} - \begin{bmatrix} \mathbf{H^F}_{ii}^{\Omega} & \mathbf{H^F}_{ib}^{\Omega} \\ \mathbf{H^F}_{bi}^{\Omega} & \mathbf{H^F}_{bb}^{\Omega} \end{bmatrix} \begin{Bmatrix} \mathbf{p}_i \\ \mathbf{p}_b \end{Bmatrix} - \\ &- \begin{bmatrix} \mathbf{M^F}_{ii}^{\Omega} & \mathbf{M^F}_{ib}^{\Omega} \\ \mathbf{M^F}_{bi}^{\Omega} & \mathbf{M^F}_{bb}^{\Omega} \end{bmatrix} \begin{Bmatrix} \dot{\mathbf{p}}_i \\ \dot{\mathbf{p}}_b \end{Bmatrix} = \begin{Bmatrix} -\mathbf{Q^F}_i + \mathbf{h^F}_i \\ -\mathbf{Q^F}_b + \mathbf{h^F}_b^{\Omega} \end{Bmatrix} \end{aligned} \tag{32}$$

- Fluid mass balance in $\Omega^+$

$$\begin{aligned} &\begin{bmatrix} \mathbf{R^F}_{bb}^{\Omega+} & \mathbf{R^F}_{be}^{\Omega+} \\ \mathbf{R^F}_{eb}^{\Omega+} & \mathbf{R^F}_{ee}^{\Omega+} \end{bmatrix} \begin{Bmatrix} \ddot{\mathbf{u}}_b \\ \ddot{\mathbf{u}}_e \end{Bmatrix} + \begin{bmatrix} \left(\mathbf{C^F}_{bb}^{\Omega+}\right)^{\mathrm{T}} & \left(\mathbf{C^F}_{be}^{\Omega+}\right)^{\mathrm{T}} \\ \left(\mathbf{C^F}_{eb}^{\Omega+}\right)^{\mathrm{T}} & \left(\mathbf{C^F}_{ee}^{\Omega+}\right)^{\mathrm{T}} \end{bmatrix} \begin{Bmatrix} \dot{\mathbf{u}}_b \\ \dot{\mathbf{u}}_e \end{Bmatrix} - \begin{bmatrix} \mathbf{H^F}_{bb}^{\Omega+} & \mathbf{H^F}_{be}^{\Omega+} \\ \mathbf{H^F}_{eb}^{\Omega+} & \mathbf{H^F}_{ee}^{\Omega+} \end{bmatrix} \begin{Bmatrix} \mathbf{p}_b \\ \mathbf{p}_e \end{Bmatrix} - \\ &- \begin{bmatrix} \mathbf{M^F}_{bb}^{\Omega+} & \mathbf{M^F}_{be}^{\Omega+} \\ \mathbf{M^F}_{eb}^{\Omega+} & \mathbf{M^F}_{ee}^{\Omega+} \end{bmatrix} \begin{Bmatrix} \dot{\mathbf{p}}_b \\ \dot{\mathbf{p}}_e \end{Bmatrix} = \begin{Bmatrix} \mathbf{Q^F}_b + \mathbf{h^F}_b^{\Omega+} \\ -\mathbf{Q^F}_e + \mathbf{h^F}_e \end{Bmatrix} \end{aligned} \tag{33}$$

The above equations must be linear in $\Omega^+$ but can be nonlinear in $\Omega$. To fulfill this condition any nonlinear constitutive model associated with the finite element in the exterior domain must work in the linear elastic mode, using stiffness parameters frozen at the initial state. The same requirement applies to flow properties $S(p)$, $c(p)$ that must also be frozen at the initial state. At this point one may assemble coresponding balance equations in the $\Omega$ and $\Omega^+$ domains and apply the following decomposition of primary variables (and their time derivatives) in the exterior domain

$$\mathbf{u}_e(t) = \mathbf{u}^o(t) + \hat{\mathbf{u}} \tag{34}$$

$$\mathbf{p}_e(t) = \underbrace{\mathbf{p}^0(t) - \mathbf{p}_e^{init}}_{\mathbf{p}^{0*}(t)} + \underbrace{\mathbf{p}_e^{init} + \tilde{\mathbf{p}}}_{\hat{\mathbf{p}}} \tag{35}$$

The $\hat{\mathbf{u}}$ and $\tilde{\mathbf{p}}$ are understood as vectors of relative values with respect to the free field. Decomposition of the pressure field in the proposed form simplifies the implementation procedure, especially if the dynamic driver is preceeded by other computational drivers (like excavation/construction etc..) generating the initial conditions. By assembling balance equations boundary forces/fluxes will disappear from the system and primary variables at nodes in the exterior domain will be replaced by $\hat{\mathbf{u}}$ and $\hat{\mathbf{p}}$

$$\begin{bmatrix} \mathbf{M}_{ii}^{\Omega} & \mathbf{M}_{ib}^{\Omega} & \mathbf{0} \\ \mathbf{M}_{bi}^{\Omega} & \mathbf{M}_{bb}^{\Omega}+\mathbf{M}_{bb}^{\Omega+} & \mathbf{M}_{be}^{\Omega+} \\ \mathbf{0} & \mathbf{M}_{eb}^{\Omega+} & \mathbf{M}_{ee}^{\Omega+} \end{bmatrix} \begin{Bmatrix} \ddot{\mathbf{u}}_i \\ \ddot{\mathbf{u}}_b \\ \ddot{\hat{\mathbf{u}}}_e \end{Bmatrix} + \begin{Bmatrix} \mathbf{F}'_{int_i} \\ \mathbf{F}'_{int_b} \\ \mathbf{0} \end{Bmatrix} + \begin{bmatrix} \mathbf{0} & \mathbf{0} & \mathbf{0} \\ \mathbf{0} & \mathbf{K}_{bb}^{\Omega+} & \mathbf{K}_{be}^{\Omega+} \\ \mathbf{0} & \mathbf{K}_{eb}^{\Omega+} & \mathbf{K}_{ee}^{\Omega+} \end{bmatrix} \begin{Bmatrix} \mathbf{u}_i \\ \mathbf{u}_b \\ \hat{\mathbf{u}}_e \end{Bmatrix} +$$
$$+ \begin{bmatrix} \mathbf{C^F}_{ii}^{\Omega} & \mathbf{C^F}_{ib}^{\Omega} & \mathbf{0} \\ \mathbf{C^F}_{bi}^{\Omega} & \mathbf{C^F}_{bb}^{\Omega}+\mathbf{C^F}_{bb}^{\Omega+} & \mathbf{C^F}_{be}^{\Omega+} \\ \mathbf{0} & \mathbf{C^F}_{eb}^{\Omega+} & \mathbf{C^F}_{ee}^{\Omega+} \end{bmatrix} \begin{Bmatrix} \mathbf{p}_i \\ \mathbf{p}_b \\ \hat{\mathbf{p}}_e \end{Bmatrix} = \begin{Bmatrix} \mathbf{0} \\ -\mathbf{M}_{be}^{\Omega+}\,\ddot{\mathbf{u}}_e^0 - \mathbf{K}_{be}^{\Omega+}\,\mathbf{u}_e^0 - \mathbf{C}_{be}^{\Omega+}\,\dot{\mathbf{u}}_e^0 - \mathbf{C^F}_{be}^{\Omega+}\,\mathbf{p}_e^{0*} \\ \mathbf{P_e} - \mathbf{M}_{ee}^{\Omega+}\,\ddot{\mathbf{u}}_e^0 - \mathbf{K}_{ee}^{\Omega+}\,\mathbf{u}_e^0 - \mathbf{C}_{ee}^{\Omega+}\,\dot{\mathbf{u}}_e^0 - \mathbf{C^F}_{ee}^{\Omega+}\,\mathbf{p}^{0*} \end{Bmatrix} \tag{36}$$

$$\begin{bmatrix} \mathbf{R^F}_{ii}^{\Omega} & \mathbf{R^F}_{ib}^{\Omega} & \mathbf{0} \\ \mathbf{R^F}_{bi}^{\Omega} & \mathbf{R^F}_{bb}^{\Omega}+\mathbf{R^F}_{bb}^{\Omega+} & \mathbf{R^F}_{be}^{\Omega+} \\ \mathbf{0} & \mathbf{R^F}_{eb}^{\Omega+} & \mathbf{R^F}_{ee}^{\Omega+} \end{bmatrix} \begin{Bmatrix} \ddot{\mathbf{u}}_i \\ \ddot{\mathbf{u}}_b \\ \ddot{\hat{\mathbf{u}}}_e \end{Bmatrix} + \begin{bmatrix} \left(\mathbf{C^F}_{ii}^{\Omega}\right)^{\mathrm{T}} & \left(\mathbf{C^F}_{ib}^{\Omega}\right)^{\mathrm{T}} & \mathbf{0} \\ \left(\mathbf{C^F}_{bi}^{\Omega}\right)^{\mathrm{T}} & \left(\mathbf{C^F}_{bb}^{\Omega}\right)^{\mathrm{T}} + \left(\mathbf{C^F}_{bb}^{\Omega+}\right)^{\mathrm{T}} & \left(\mathbf{C^F}_{be}^{\Omega+}\right)^{\mathrm{T}} \\ \mathbf{0} & \left(\mathbf{C^F}_{eb}^{\Omega+}\right)^{\mathrm{T}} & \left(\mathbf{C^F}_{ee}^{\Omega+}\right)^{\mathrm{T}} \end{bmatrix} \begin{Bmatrix} \dot{\mathbf{u}}_i \\ \dot{\mathbf{u}}_b \\ \dot{\hat{\mathbf{u}}}_e \end{Bmatrix} -$$
$$\begin{bmatrix} \mathbf{H^F}_{ii}^{\Omega} & \mathbf{H^F}_{ib}^{\Omega} & \mathbf{0} \\ \mathbf{H^F}_{bi}^{\Omega} & \mathbf{H^F}_{bb}^{\Omega}+\mathbf{H^F}_{bb}^{\Omega+} & \mathbf{H^F}_{be}^{\Omega+} \\ \mathbf{0} & \mathbf{H^F}_{eb}^{\Omega+} & \mathbf{H^F}_{ee}^{\Omega+} \end{bmatrix} \begin{Bmatrix} \mathbf{p}_i \\ \mathbf{p}_b \\ \hat{\mathbf{p}}_e \end{Bmatrix} - \begin{bmatrix} \mathbf{M^F}_{ii}^{\Omega} & \mathbf{M^F}_{ib}^{\Omega} & \mathbf{0} \\ \mathbf{M^F}_{bi}^{\Omega} & \mathbf{M^F}_{bb}^{\Omega}+\mathbf{M^F}_{bb}^{\Omega+} & \mathbf{M^F}_{be}^{\Omega+} \\ \mathbf{0} & \mathbf{M^F}_{eb}^{\Omega+} & \mathbf{M^F}_{ee}^{\Omega+} \end{bmatrix} \begin{Bmatrix} \dot{\mathbf{p}}_i \\ \dot{\mathbf{p}}_b \\ \dot{\hat{\mathbf{p}}}_e \end{Bmatrix} =$$
$$\begin{Bmatrix} -\mathbf{Q^F}_i + \mathbf{h^F}_i \\ \mathbf{h^F}_b^{\Omega} + \mathbf{h^F}_b^{\Omega+} \\ \mathbf{h^F}_e \end{Bmatrix} + \begin{Bmatrix} \mathbf{0} \\ -\mathbf{R^F}_{be}^{\Omega+}\,\ddot{\mathbf{u}}_e^0 - \left(\mathbf{C^F}_{be}^{\Omega+}\right)^{\mathrm{T}}\dot{\mathbf{u}}_e^0 + \mathbf{H^F}_{be}^{\Omega+}\,\mathbf{p}^{0*} + \mathbf{M^F}_{be}^{\Omega+}\,\dot{\mathbf{p}}^{0*} \\ -\mathbf{Q^F}_e - \mathbf{R^F}_{ee}^{\Omega+}\,\ddot{\mathbf{u}}_e^0 - \left(\mathbf{C^F}_{ee}^{\Omega+}\right)^{\mathrm{T}}\dot{\mathbf{u}}_e^0 + \mathbf{H^F}_{ee}^{\Omega+}\,\mathbf{p}^{0*} + \mathbf{M^F}_{ee}^{\Omega+}\,\dot{\mathbf{p}}^{0*} \end{Bmatrix} \tag{37}$$

The $\mathbf{P}_e$ and $\mathbf{Q}_e$ terms can now be derived from eq.(31), and eq.(33) respectively, assuming that these are solved for a simpler problem that does not include the structure

$$\mathbf{P}_e = \mathbf{M}_{eb}^{\Omega+}\ddot{\mathbf{u}}_b^0 + \mathbf{M}_{ee}^{\Omega+}\ddot{\mathbf{u}}_e^0 + \mathbf{K}_{eb}^{\Omega+}\mathbf{u}_b^0 + \mathbf{K}_{ee}^{\Omega+}\mathbf{u}_e^0 + \mathbf{C^F}_{eb}^{\Omega+}\mathbf{p}_b^{0*} + \mathbf{C^F}_{ee}^{\Omega+}\mathbf{p}_e^{0*} \tag{38}$$

$$-\mathbf{Q}_e = -\mathbf{h^F}_e + \mathbf{R^F}_{eb}^{\Omega+}\ddot{\mathbf{u}}_b^0 + \mathbf{R^F}_{ee}^{\Omega+}\ddot{\mathbf{u}}_e^0 + \left(\mathbf{C^F}_{eb}^{\Omega+}\right)^{\mathrm{T}}\dot{\mathbf{u}}_b^0 + \left(\mathbf{C^F}_{ee}^{\Omega+}\right)^{\mathrm{T}}\dot{\mathbf{u}}_e^0 - \mathbf{H^F}_{eb}^{\Omega+}\mathbf{p}_b^{0*} - \mathbf{H^F}_{ee}^{\Omega+}\mathbf{p}_e^{0*} - \mathbf{M^F}_{eb}^{\Omega+}\dot{\mathbf{p}}_b^{0*} - \mathbf{M^F}_{ee}^{\Omega+}\dot{\mathbf{p}}_e^{0*} \tag{39}$$

As the method is implemented in the finite element framework we need to select at least a single row of finite elements, in the reduced model, that is treated as a boundary layer separating the interior and exterior domains. One may easily notice that these extra terms on the right hand side are computed only within the layer of elements in boundary domain. Starting from the above equations one may linearize them and apply any time integration scheme (Newmark, HHT or any other). The method was implemented within the ZSOIL code (Elmepress and Zace Services Limited 2013) starting with version ZSOIL.PC 2013.

## 4 NUMERICAL EXAMPLE

To verify DRM method an example of twin tunnels (see Fig.(2(a))) subject to the scaled (by factor 0.2) Loma Prieta (see Fig. 2(b)) acceleration record (record shown in the figure is not scaled), is analyzed. In this example two dynamic models are considered, a rigid base (run in relative displacements) and compliant base one (run in the absolute). For the rigid base model bedrock is assumed to be infinitely stiff and hence depth of the model is 30m while for the compliant base model a 15m layer of a bedrock is added. In the latter model, at the bottom, boundary viscous dashpots are added and excitation is transfered through the viscous tractions computed based on velocities integrated via Newmark scheme from given acceleration record (Mejia & Dawson 2006). The free field motions for both dynamic models are computed for a simple shear layer assuming that subsoil is fully saturated while bedrock is an impermeable material (in compliant base model). The shear layer model is discretized using Q4-BBAR elements assuming periodic boundary conditions for displacements and pore pressures (only one element along the $L_1$ dimension is used) (see Fig.3(a), Fig.3(c)). In both reduced models (see Fig.3(b), Fig.3(d)), at external edges of the exterior domain, viscous dashpots are added. In both dynamic models the scaled acceleration record is assumed to be given at the base of the model (in case of compliant base model no deconvolution procedure was carried out to transfer the signal from top layer of the bedrock to the base). In the implementation we assume that mesh in the reduced model must be fully overlapped by the mesh of the background model (shear layer mesh in considered cases). To study the accuracy of the method with respect to the size of the reduced model dimension $L_2$ three computations were run, for $L_2 = 280$ m, $L_2 = 160$ m and $L_2 = 100$ m, for both dynamic models. Subsoil is modeled as nonlinear elastic-plastic Mohr-Coulomb model in which stiffness Young modulus at low strains is a power function of current mean effective stress $p'$ according to the formula $E = E_o \left( \frac{p'}{\sigma_{ref}} \right)^m$. Material properties for subsoil are as follows: $E_o = 300000$ MPa, $\nu = 0.2$, $m = 0.5$, $\phi = 27^o$, $c = 5$ kPa, $k = 10^{-7}$ m/s, $S_r = 0.0$, $\alpha = 0.1$ m$^{-1}$, $\gamma_{dry} = 17$ kN/m$^3$, $e_o = 0.559$. Low frequency damping is activated for subsoil using Rayleigh mass proportional damping with factor $\alpha_o = 1.257$ that corresponds to the 5% damping at frequency 2Hz. Tunnel lining is modeled as an elastic beam with section depth of 30 cm and elastic parameters $E = 30000000$ kPa, $\nu = 0.2$, with zero damping. Bedrock in the compliant base model is assumed to be an elastic material characterized by $E = 1000000$, kPa, $\nu = 0.3$, $\gamma = 23$ kN/m$^3$ with zero damping. The averaged Q4-BBAR element size is 1.2m while the applied time step $\Delta t = 0.01$ s. The HHT scheme was used in all cases ($\alpha = -0.3$). All dynamic time history analyses for reduced models (models that include the structure) were preceeded by static two-phase uncoupled analyses consisting of the initial state (assuming $K_o^{insitu} = 0.7$) and then the excavation/construction step during which tunnel lining was installed. This requires special procedures to handle adding/removing boundary conditions and ability to preserve remaining reactions. This option is standard in the ZSOIL code.

Horizontal displacement time history at point A for rigid base model is shown in Fig.4(a). One may notice that for $L_1 = 280$m and $L_1 = 160$m during first 5s of shaking quite a good agreement is achieved. Later on certain deviation is observed. Additional computations, carried out for a rigid base model with larger value of damping parameter $\alpha_o = 2.512$, show much beter agreement for cases $L_1 = 280$m and $L_1 = 160$m while for $L_1 = 100$ m still some deviations are observed. These observed deviations are caused by the assumption of a rigid base that causes lot of reflections if damping is too low, but also by the fact that paraxial viscous dashpots cannot fully absorb incoming waves. This spurious effects are well visible at end of shaking when

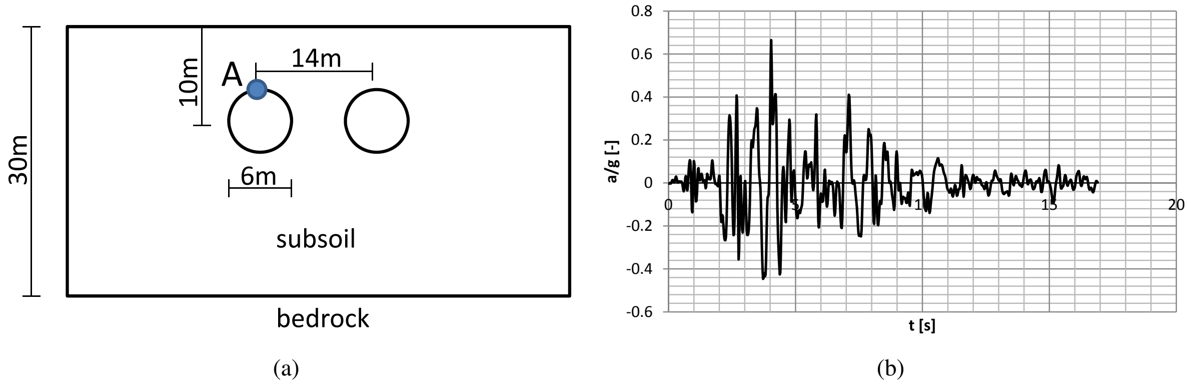


Fig. 2. Data setup. (a) Geometry of the problem. (b) Baseline corrected and filtered (10 Hz low pass Butterworth filter) original Loma Prieta acceleration record (18.10.1989 Corralitos station)).

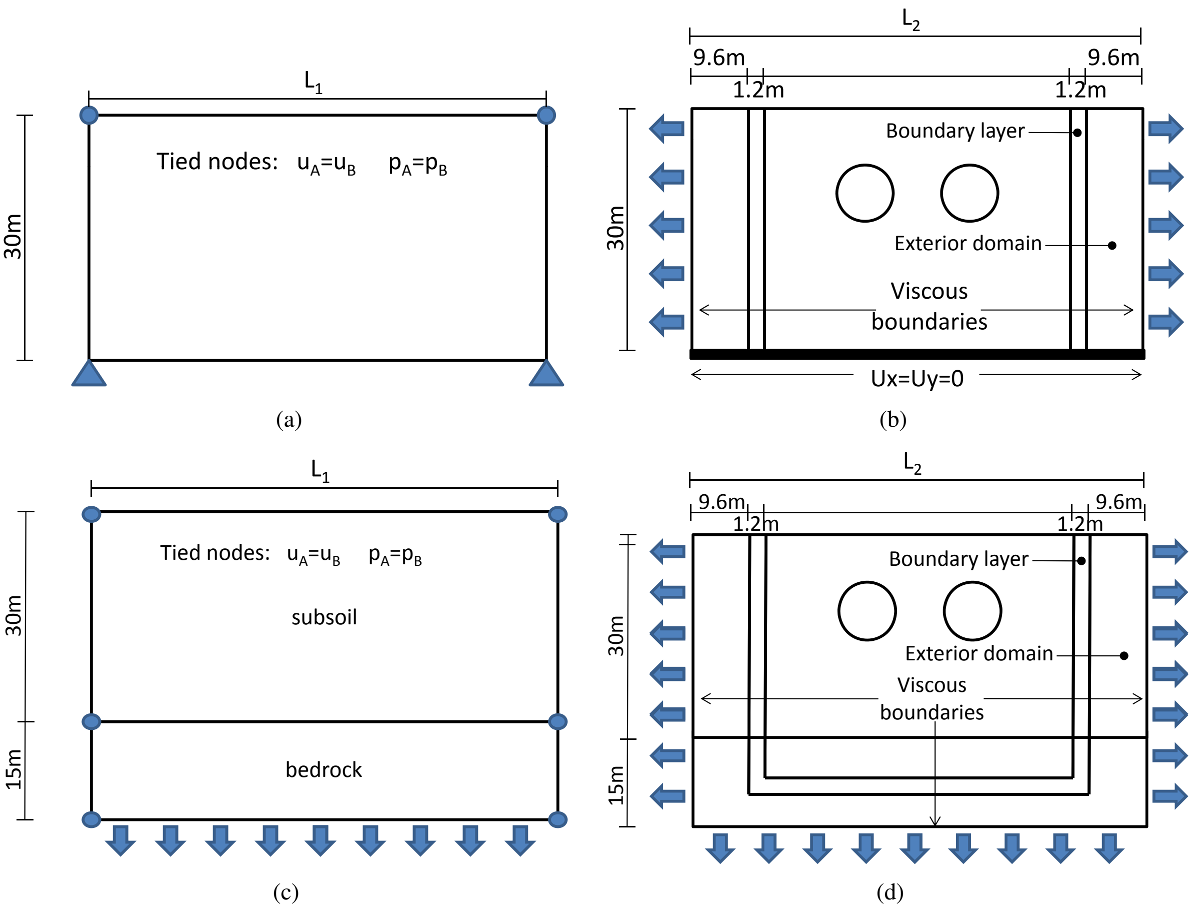


Fig. 3. Data setup. (a) Free field model for rigid base assumption. (b) Reduced model for rigid base assumption. (c) Free field model for compliant base assumption. (d) Reduced model for compliant base assumption.

displacement amplitudes are still large. Computations carried out for compliant base model show an excellent agreement for all three reduced models (see Fig.4(a)).

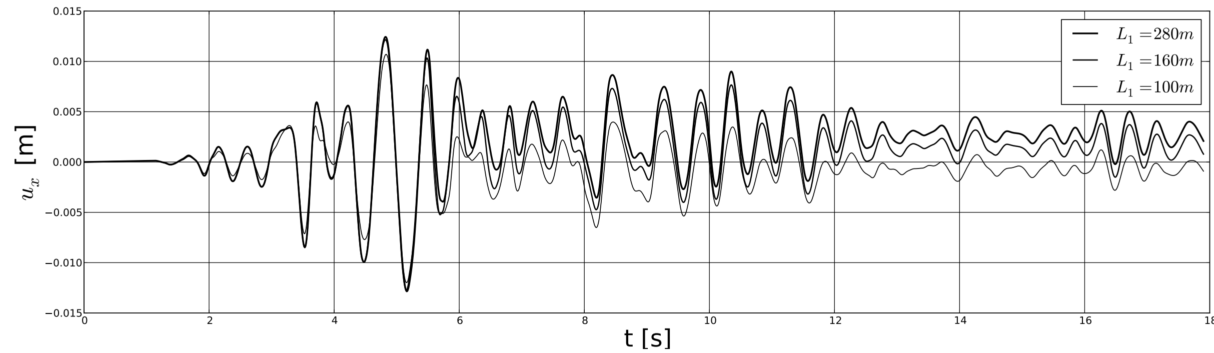


(a)

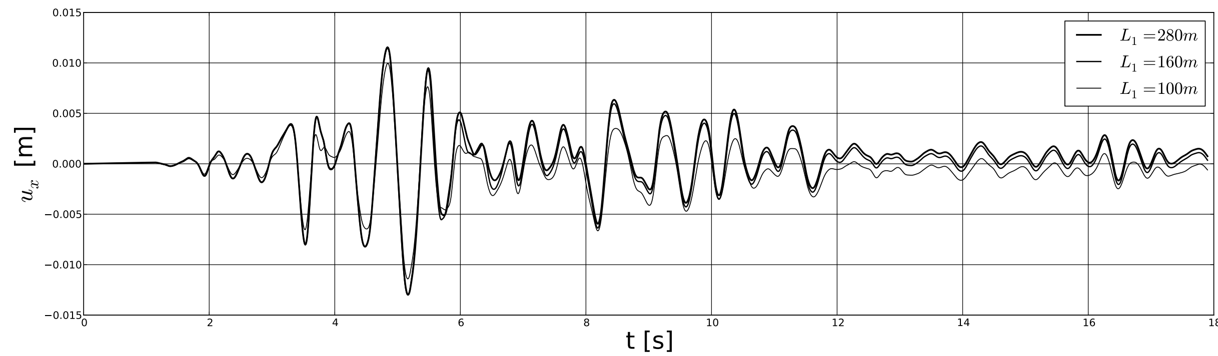


(b)

Fig. 4. $u_x$ time histories at point A for rigid base model. (a) Damping parameter $\alpha_o = 1.256$. (b) Damping parameter $\alpha_o = 2.512$.

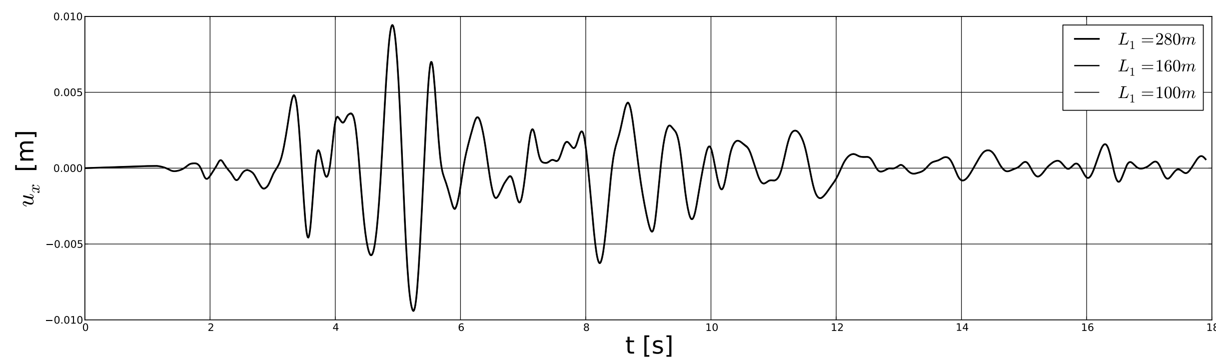


Fig. 5. $u_x$ time histories at point A for compliant base model (damping parameter $\alpha_o = 1.256$).

## 5 CONCLUSIONS

Although DRM method is applicable to linear and nonlinear problems, the free field motion must be analyzed as a linear one. The benefit of the method is such that only a relatively small part of the subsoil, adjacent to the structure, needs to be included in the analysis. Moreover, the spatial dimension of a free field motion problem can be lower than the one of the reduced model (structure plus small adjacent subsoil zone). Typically, one may find the free field motion from a 1D shear layer model and then analyze the 2D/3D soil-structure interaction based on this simple free field solution. Proper selection of the size of the reduced model, dimensions of the exterior domain for complex soil models in mixed saturated/partially saturated conditions is still an open issue and requires more research. The compliant base model shows much better behavior compared to the rigid base model that causes lots of spurious wave reflections from rigid boundary. This model combined with the DRM method proves to be a robust tool for solving nonlinear soil-structure interaction problems.

## REFERENCES

Aubry, D. & Ozanam, O. (1988). Free-surface tracking through non-saturated models. In Swoboda (Ed.), *Numerical Methods in Geomechanics*, Innsbruck, pp. 757–763. Balkema.

Bielak, J., Loukakis, K., Hisada, Y., & Youshimura, C. (2003). Domain reduction method for three-dimensional earthquake modeling in localized regions. part i: Theory. *Bulletin of the seismological Society of America 93*, 817–824.

Elmepress and Zace Services Limited (1985-2013). *Z_SOIL manual*. Lausanne, Switzerland: Elmepress and Zace Services Limited.

Genuchten, V. (1980). A closed form equation for predicting the hydraulic conductivity of unsaturated soils. *Soil Sciences Am. Soc. 44*, 892–898.

Hilber, H. M., Hughes, T. J. R., & Taylor, R. L. (1977). Improved numerical dissipation for time integration algorithms in structural dynamics. *Earthquake Engineering & Structural Dynamics 5*, 283–292.

Irmay, S. (1956). On the hydraulic conductivity of unsaturated soils. *Trans. Am. Geophys. Union 35*, 463–468.

Kantoe, S. (2006, May). *Development of time integration schemes and advanced boundary conditions for dynamic analysis*. Ph. D. thesis, Department of Civil and Environmental Engineering, Imperial College of Science, Technology and Medicine, London, SW7 2BU.

Kantoe, S., Zdravkovic, L., & Potts, D. (2008). The domain reduction method for dynamic coupled consolidation problems in geotechnical engineering. *International Journal for Numerical and Analytical Methods in Geomechanics 32*, 659–680.

Mejia, L. & Dawson, E. (2006). Earthquake deconvolution for FLAC. paper 04-10. In *4th International FLAC Symposium on Numerical Modeling in Geomechanics*, Minneapolis, pp. 2–9.

Modaressi, H. & Benzenati, I. (1994). Paraxial approximation for poroelastic media. *Soil Dynamics and Earthquake Engineering 13*, 117–129.

Truty, A. & Zimmermann, T. (2006). Stabilized mixed finite element formulations for materially nonlinear partially saturated two-phase media. *Computer Methods in Applied Mechanics and Engineering 195*, 1517–1546.

Youshimura, C., Bielak, J., Hisada, Y., & Fernandez, A. (2003). Domain reduction method for three-dimensional earthquake modeling in localized regions. part ii: Verification and applications. *Bulletin of the seismological Society of America 93*, 825–840.

Zienkiewicz, O., Chan, A., Pastor, M., Schrefler, B., & Shiomi, T. (1999). *Computational Geomechanics with Special Reference to Earthquake Engineering*. John Wiley & Sons Ltd.